Int. J. Environ. Sci. Technol. (2012) 9:319–326
DOI 10.1007/s13762-012-0045-7

ORIGINAL PAPER

Hexavalent chromium removal from aqueous solutions by using low-cost biological wastes: equilibrium and kinetic studies

M. Aliabadi · I. Khazaei · H. Fakhraee · M. T. H. Mousavian

Received: 4 January 2011 / Revised: 25 September 2011 / Accepted: 28 November 2011 / Published online: 20 March 2012

Abstract The batch removal of hexavalent chromium from aqueous solutions using almond shell, activated sawdust, and activated carbon, which are low-cost biological wastes under different experimental conditions, was investigated in this study. The influences of initial concentration, adsorbent dose, adsorbent particle size, agitation speed, temperature, contact time, and pH of solution were investigated. The adsorption was solution pH dependent and the maximum adsorption was observed at a solution pH of 2.0. The capacity of chromium adsorption under equilibrium conditions increased with the decrease in particle sizes. The equilibrium was achieved for chromium ion after 30 min. Experimental results showed that low-cost biosorbents are effective for the removal of pollutants from aqueous solution. The pseudo-second-order kinetic model gave a better fit of the experimental data as compared to the pseudo-first-order kinetic model. Experimental data showed a good fit with the Freundlich isotherm model. Changes in the thermodynamic parameters, including Gibbs free energy (ΔG_o), enthalpy (ΔH_o), and entropy (ΔS_o), indicated that the biosorption of hexavalent chromium onto almond shell, activated sawdust, and activated carbon was feasible, spontaneous, and endothermic in the temperature range 28–50 °C.

Keywords Activated sawdust · Almond shell · Biosorption · Endothermic · Modeling

M. Aliabadi (✉) · I. Khazaei
Department of Chemical Engineering,
Islamic Azad University, Birjand Branch,
Birjand, Iran
e-mail: majid.aliabadi@gmail.com

H. Fakhraee
Department of Civil Engineering,
Iran University of Science and Technology,
Tehran, Iran

M. T. H. Mousavian
Department of Chemical Engineering,
Ferdowsi University of Mashhad,
Mashhad, Iran

Introduction

Hexavalent chromium (Cr(VI)) is a high priority pollutant and has been identified as a carcinogen (Hasany and Chaudhary 1998). Heavy metals are widely used by modern industries, including textile, leather, tanning, electroplating, and metal finishing. Cr(VI) is typically found in wastewaters (such as electroplating or leather tanning wastewaters) in the concentration range 50–100 mg/L (Xi et al. 1996). As with other heavy metals, trace amounts of chromium are necessary for life processes.

However, higher concentration of this element in the environment is toxic and can result in a variety of animal diseases such as dermatitis, congestion of respiratory tracts, and perforation of the nasal septum. Because of its high toxicity, it is imperative to significantly reduce its discharge levels (Bianchi and Levis 1984). Many methods have been used for removal of heavy metals in wastewaters such as reverse osmosis (Ozaki et al. 2002), ion exchange (Zhang et al. 2010), membrane separation (Kozlowski and Walkowiak 2002; Shaalan et al. 2001), chemical precipitation, and electrolysis (Tunali Akar et al. 2009). Among these, the adsorption method is superior because of its higher efficiency and simple operation (Bailey et al. 1999).

Different types of biosorbents have been investigated for the removal of heavy metals from aqueous solutions (Abdel-Ghani and El-Chaghaby 2007; Okoye et al. 2010;

Wuana et al. 2010; Zavvar Mousavi and Seyedi 2011; Gueu et al. 2007). Among many biosorbents naturally available, plant biomass can be used as an inexpensive biosorbent for removal of metal ions from synthetic solutions and industrial effluents (Manal 2007).

In this study, almond shell, activated sawdust, and activated carbon were used for removal of Cr(VI) from aqueous solution; the influences of operating conditions such as contact time, initial concentration, pH, temperature, agitation speed, adsorbent dose, and particle size were investigated. The experiments were conducted in the Department of Chemical Engineering, Birjand Branch, Islamic Azad University, during 2009–2010.

Materials and methods

The almond shell was taken from local natural resources. Before use, it was washed with deionised water to remove surface impurities and dried at 100 °C. The material was ground to a fine powder in a still mill. The resulting material was sieved in the size range >20, <30, and >30 mesh ASTM, and stored in plastic bottle for further use. The sawdust of the aspen tree was prepared from local agricultural solid wastes in Birjand, Iran. Sawdust was soaked with 1 M HCL solutions for 30 min, rinsed several times with deionised water, oven dried at 100 °C and used as activated sawdust. Samples were ground in a blender to use for adsorption experiments.

Potassium dichromate and other chemicals were purchased from Merck Co. Ltd. (Darmstadt, Germany). Activated carbon was purchased from Carbokarn Co. Ltd. (Bangkok, Thailand). The physical properties of activated carbon are listed in Table 1.

Adsorbent preparation

A known weight of adsorbent (2.0 g) was equilibrated with 100 mL of the chromium solution of known concentration (5 mg/L) in a 250 mL glass flask at 25 ± 2 °C. Chromium solution was prepared by dissolving potassium dichromate ($K_2Cr_2O_7$) in distilled water. Fresh dilutions were used for each experiment. The pH of the solution was adjusted with 0.1 N NaOH or 0.1 N HCl.

Table 1 Physical properties of activated carbon (type PHO 8/35 LBD)

Property	Value
Particle size (mm)	0.50–2.36
Surface area ($m^2\ g^{-1}$)	900–1,100
Solid density ($g\ cm^{-3}$)	0.48
Packing density ($g\ cm^{-3}$)	0.53
Pore volume ($mL\ g^{-1}$)	0.73

The mixtures were agitated at a speed of 400 rpm on a mechanical shaker for 30 min to reach equilibrium. After equilibrium, all sample solutions were filtered through a 0.45 μm membrane filter and their concentrations were analyzed by a spectrophotometer (JENWAY 6305 UV/Vis model) using 1,5-diphenylcarbazide as the complexing agent at the wavelength of 540 nm (Arthur and Vogel 1978).

The Cr(VI) loadings on adsorbent were computed from the difference in Cr(VI) concentrations in aqueous solution before and after the addition of adsorbent. The effects of several parameters, such as contact time, initial concentration, pH, temperature, agitation speed, adsorbent dose, and particle size on extent of adsorption of Cr(VI) were investigated. The adsorption capacity and intensity were modeled by the Langmuir, Freundlich, and Temkin isotherms.

The amount of Cr(VI) adsorbed and the percentage removal of Cr(VI) were calculated using Eqs. 1 and 2, respectively.

$$q_e = \frac{(C_\circ - C_e)V}{M} \quad (1)$$

$$\%\ \text{Removal of Cr(VI)} = \frac{C_i - C_o}{C_i} \times 100 \quad (2)$$

where q_e is the adsorption capacity in mg/g, C_i, C_o and C_e are the initial, outlet and equilibrium concentration of Cr(VI) in mg/L, V is the volume of Cr(VI) solution in L, and M is the weight of the adsorbent in g (Feng and Aldrich 2004).

Results and discussion

Effect of contact time

Figure 1 shows the percentage of removal of Cr(VI) by almond shell, activated sawdust, and activated carbon, as a function of time. The experiments were carried out at 25 ± 2 °C, with 2 g of adsorbent with particle size of <30 mesh, in 100 mL of chromium solution and initial Cr(VI) concentration of 5 mg/L. It can be seen from Fig. 1 that the percentage of removal of Cr(VI) initially rises rapidly with time (up to 15 min) but then the rate of rise drops and approaches a constant rate.

This may be explained by the fact that the biosorption sites are open at the beginning of the biosorption process, so Cr(VI) interacts easily with these sites. As time goes on, the biosorption sites became saturated with Cr(VI) and the concentration of Cr(VI) in liquid phase remains almost constant.

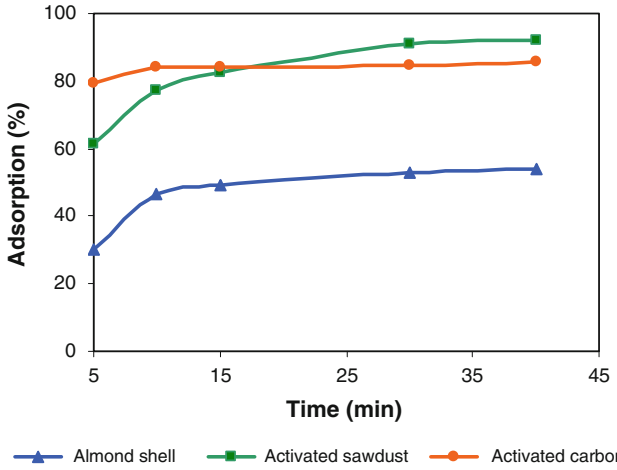

Fig. 1 Effect of contact time on the removal of Cr(VI) (initial Cr(VI) concentration = 5 mg/L, adsorbent dose = 2 g 100^{-1} mL, temperature = 26 °C, agitation speed = 400 rpm)

In order to make sure whether sufficient contact time was obtained, further biosorption experiments were carried out for 30 min.

Effect of initial Cr(VI) concentration

The percentage of adsorption of Cr(VI) with different adsorbents was studied by varying Cr(VI) concentration in the range 0.5–5 mg/L. As shown in Fig. 2, the percentage of removal decreased with increase in Cr(VI) concentration. At low Cr(VI) concentrations, the ratio of available adsorbent surface to the initial Cr(VI) concentration is larger, and therefore, the removal is independent of initial concentrations. However, at higher Cr(VI) concentrations, this ratio is low and the percentage of removal then depends upon the initial concentration. The results show that within a certain range of initial metal concentration, the percentage of metal adsorption on adsorbent is determined by the adsorption capacity of the adsorbent.

Table 2 Effect of adsorbent dose on the removal of Cr(VI) (initial Cr(VI) concentration = 5 mg/L, temperature = 26 °C, agitation speed = 400 rpm, contact time = 30 min)

Adsorbent dose (gr)	Almond shell (% adsorption)	Activated sawdust (% adsorption)	Activated carbon (% adsorption)
1	29.7	63.2	80.2
2	53.1	90.8	84.6
3	61.1	97.6	85.2
4	66.5	97.9	85.3
6	75.9	98.1	86.1

Effect of adsorbent dose

The effect of adsorbent dose on Cr(VI) uptake was investigated by varying the adsorbent dose (Table 2). Experimental results showed that the percentage of removal of Cr(VI) increases with the increasing amount of adsorbent. This can be explained by the fact that with increase in the mass of adsorbent, the available surface for adsorption of Cr(VI) also increases.

Effect of pH

The pH of the aqueous solution is an important controlling parameter in the adsorption process. As the results show, adsorption of Cr(VI) was higher at lower pH and decreased with increasing pH (Fig. 3). Maximum adsorption was obtained at initial pH of 2.0.

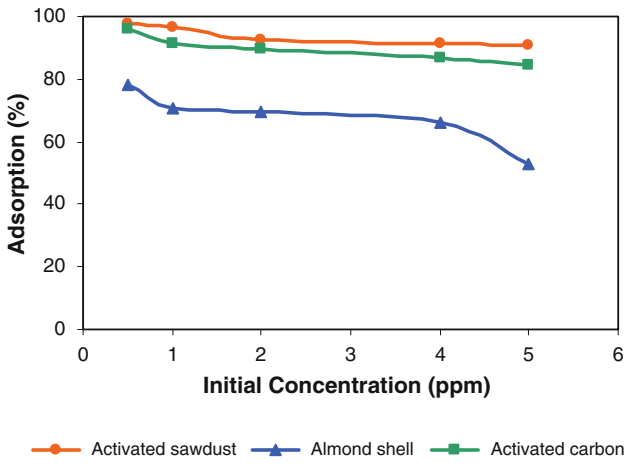

Fig. 2 Effect of initial Cr(VI) concentration on the removal of Cr(VI) (adsorbent dose = 2 g 100^{-1} mL, temperature = 26 °C, agitation speed = 400 rpm, contact time = 30 min)

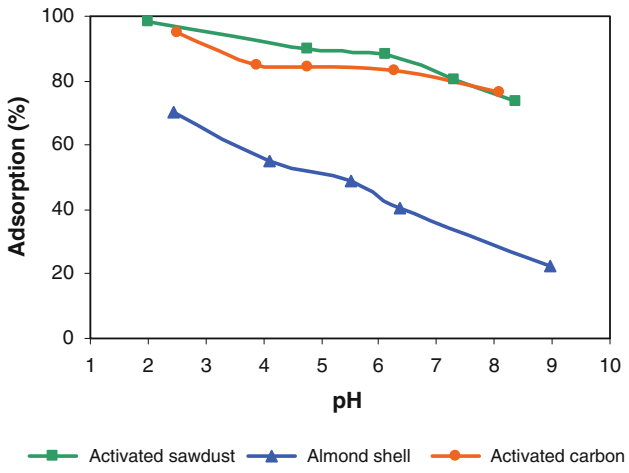

Fig. 3 Effect of pH on the removal of Cr(VI) (initial Cr(VI) concentration = 5 mg/L, temperature = 26 °C, adsorbent dose = 2 g 100^{-1} mL, agitation speed = 400 rpm, contact time = 30 min)

The chromium compounds at pH = 2 are $HCrO_4^-$ (CrO_4^{-2}) and also $Cr_2O_7^{-2}$, with the former being the dominant form.

At pH = 2, due to the excess amount of H^+ ions within the medium, the active sites on the adsorbent become positively charged. This causes a strong attraction between these sites and negatively charged $HCrO_4$ ions:

$$\equiv OH_2^+ + HCrO_4^- \leftrightarrow OH_2^+(HCrO_4^-) \quad (3)$$

As a result, adsorption of negative metals increases significantly. When pH value increases, surface of the adsorbent becomes neutral and chromium adsorption reduces. When the adsorbent surface is negatively charged, adsorption decreases significantly. This behavior is specific to the chromium ions and it is different for the divalent metals. Chromium ions release hydroxide ions to the solution instead of proton (Muradiye and Irfan 2007).

Effect of temperature

The adsorption of Cr(VI) increases when the temperature is increased (Fig. 4). This shows that the adsorption reaction is endothermic in nature. The enhancement in the adsorption capacity may be due to the chemical interaction between adsorbates and adsorbent, creation of some new adsorption sites or the increased rate of intraparticle diffusion of Cr(VI) ions into the pores of the adsorbent at higher temperatures.

Kinetic energy of the chromium ions is low at low temperatures and therefore, under these conditions, it is very difficult and time-consuming process for ions to reach the active sites on the adsorbent. Increase in temperature causes increase in the mobility of the ions. If temperature is further increased, the kinetic energy of chromium ions becomes more than the potential attractive forces between active sites and ions.

Table 3 Effect of particle size on the removal of Cr(VI) (initial Cr(VI) concentration = 5 mg L^{-1}, temperature = 26 °C, adsorbent dose = 2 g 100^{-1} mL, agitation speed = 400 rpm, contact time = 30 min)

Particle size (mesh number)	Almond shell (% adsorption)	Activated sawdust (% adsorption)	Activated carbon (% adsorption)
>20	53.1	90.8	84
<30	53.9	93.2	85.4
>30	68.2	97.9	86.7

Effect of particle size

The effect of particle size on Cr(VI) adsorption capacity of almond shell, activated sawdust, and activated carbon is shown in Table 3. The removal of Cr(VI) ions at different particle sizes indicated that the capacity of chromium adsorption at the equilibrium increased with the decrease in particle sizes. The relatively higher adsorption with smaller adsorbent particle may be attributed to the fact that smaller particles yield large surface areas and shows that chromium ion adsorption occurs through a surface mechanism. It can also be observed that smaller particles reach equilibration faster.

Effect of agitation speed

The rate of mass transfer of chromium ions from the solution to the solid surface depends to some extent on the degree of mixing. The chromium removal curve presented in Fig. 5

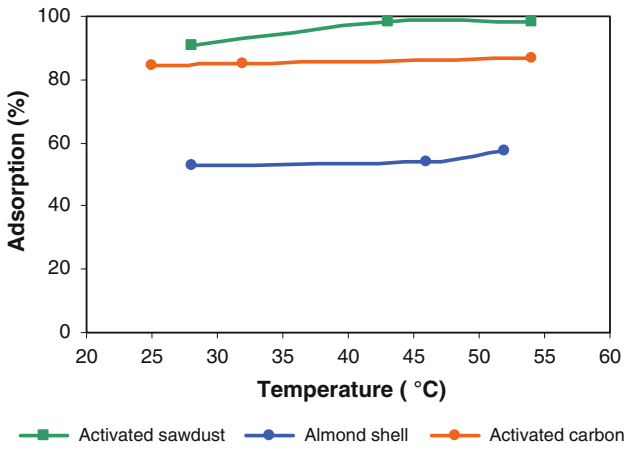

Fig. 4 Effect of temperature on the removal of Cr(VI) (initial Cr(VI) concentration = 5 mg/L, adsorbent dose = 2 g 100^{-1} mL, agitation speed = 400 rpm, contact time = 30 min)

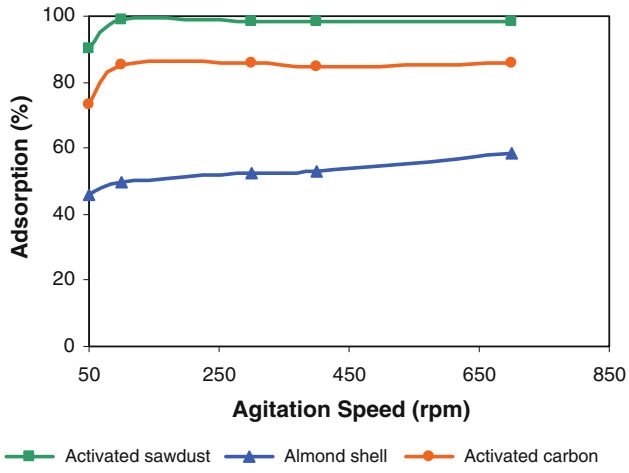

Fig. 5 Effect of agitation speed on the removal of Cr(VI) (initial Cr(VI) concentration = 5 mg/L, temperature = 26 °C, adsorbent dose = 2 g 100^{-1} mL, contact time = 30 min)

indicates that at lower degree of agitation, the effect of mass transfer is pronounced, but the effect becomes insignificant at higher degrees of agitation. At higher degree of agitation, the effect of mass transfer is present at the beginning of the process while its effect diminishes with time.

Adsorption isotherm

Adsorption equilibrium data were fitted to the Langmuir, Freundlich, and Temkin isotherms.

Langmuir isotherm model

The Langmuir isotherm is based on the monolayer adsorption of chromium ions on the surface of adsorbent sites and is expressed in the linear form in Eq. 4 (Aliabadi et al. 2006).

$$\frac{C_e}{x/m} = \frac{1}{KV_m} + \frac{C_e}{V_m} \quad (4)$$

where C_e is the equilibrium solution concentration, x/m the amount adsorbed per unit mass of adsorbent, m the mass of the adsorbent, V_m the monolayer capacity, and K is equilibrium constant related to the heat of adsorption by Eq. 5:

$$K = K_0 \times \exp\left(\frac{q}{RT}\right) \quad (5)$$

where q is the heat of adsorption.

Freundlich isotherm model

The Freundlich isotherm describes the heterogeneous surface energies by multilayer adsorption and is expressed in linear form in Eq. 6 (Aliabadi et al. 2006):

$$\log\frac{x}{m} = \log K_f + \frac{1}{n}\log C_e \quad (6)$$

where K_f and $1/n$ are Freundlich constants related to adsorption capacity and intensity of adsorption, and other parameters are the same as in the Langmuir isotherm. The term $\log(x/m)$ can be plotted against $\log C_e$ with slope $1/n$ and intercept $\log K_f$.

Temkin isotherm model

The Temkin isotherm is based on the heat of adsorption of ions and is presented in linear form, in Eq. 7 (Karthikeyan et al. 2005):

$$\frac{x}{m} = \left(\frac{RT}{b}\right)\ln A + \left(\frac{RT}{b}\right)\ln C_e$$
$$\frac{RT}{b} = B \quad (7)$$

where b is the Temkin constant related to heat of sorption (J/mol), A the Temkin isotherm constant (L g^{-1}), R the gas constant (8.314 J $(mol\ K)^{-1}$), and T is the absolute temperature (K).

The data obtained from the adsorption experiments conducted at 25 ± 2 °C were fitted to Eqs. 4, 6, and 7 and linear plots (not shown) were obtained for $C_e/(x/m)$ versus C_e, $\log(x/m)$ versus $\log(C_e)$ and x/m versus $\ln C_e$, respectively. The theoretical parameters of isotherms along with regression coefficient are shown in Table 4.

The three isotherms are compared with each other in Figs. 6, 7, and 8.

According to Table 4 and Figs. 6, 7, and 8, the Freundlich equation fits the experimental data better than the Langmuir and Timken equations do.

Table 4 Isotherm constants for various adsorption isotherms

Adsorbent name	Langmuir constants		
	V_m (mg/g)	K (mg/L)	R^2
Almond shell	0.210	0.846	0.924
Activated carbon	0.310	2.470	0.886
Activated sawdust	0.261	7.616	0.789
Adsorbent name	**Freundlich constants**		
	$1/n$	K_f (mg/g)	R^2
Almond shell	0.680	0.089	0.969
Activated carbon	0.611	0.240	0.987
Activated sawdust	0.574	0.324	0.989
Adsorbent name	**Temkin constants**		
	B	A (L g^{-1})	R^2
Almond shell	0.042	11.129	0.927
Activated carbon	0.051	48.594	0.885
Activated sawdust	0.051	98.970	0.871

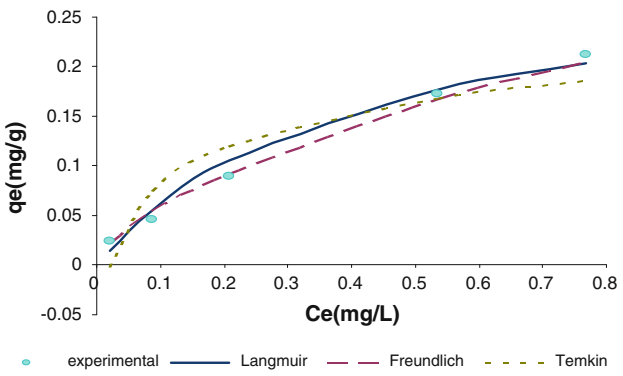

Fig. 6 Equilibrium isotherms of Cr(VI) on to activated carbon (temperature = 26 °C, adsorbent dose = 2 g 100^{-1} mL, agitation speed = 400 rpm, contact time = 30 min)

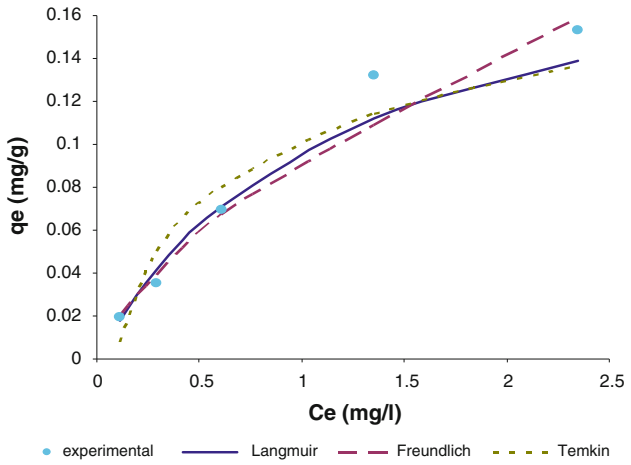

Fig. 7 Equilibrium isotherms of Cr(VI) on to almond shell (temperature = 26 °C, adsorbent dose = 2 g 100^{-1} mL, agitation speed = 400 rpm, contact time = 30 min)

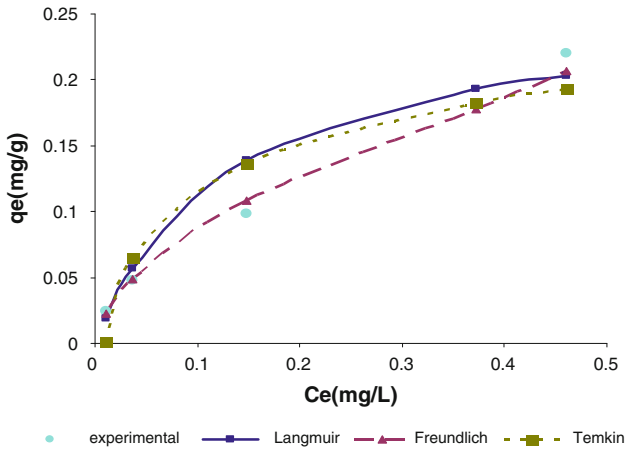

Fig. 8 Equilibrium isotherms of Cr(VI) on to activated sawdust (temperature = 26 °C, adsorbent dose = 2 g 100^{-1} mL, agitation speed = 400 rpm, contact time = 30 min)

Adsorption kinetics modeling

To find the potential rate-controlling steps involved in the process of biosorption of Cr(VI) onto almond shell, activated sawdust and activated carbon, both pseudo-first-order and pseudo-second-order kinetic models were used to fit the experimental data.

Pseudo-first-order model

The pseudo-first-order kinetic model was described by Lagergren 1898:

$$\frac{dq}{dt} = k_1(q_e - q_t) \tag{8}$$

where q_e (mg/g) and q_t (mg/g) are the amounts of the Cr(VI) adsorbed on the adsorbent at equilibrium and at time t, respectively; and k_1 (min^{-1}) is the rate constant of the first-order model. After integration and applying boundary conditions: $q_t = 0$ at $t = 0$ and $q_t = q_t$ at $t = t$, the integrated form of Eq. 8 becomes:

$$\ln(q_e - q_t) = \ln q_e - k_1 t \tag{9}$$

A straight line of $\ln(q_e - q_t)$ versus t suggests the applicability of this kinetic model; q_e and k_1 can be determined from the intercept and slope of the plot, respectively.

It is important to note that the experimental q_e must be known for the application of this model. Table 5 shows the pseudo-first-order constants, q_e and k_1, along with the corresponding correlation coefficients for initial Cr(VI) concentration of 5 mg/L. The calculated $q_{e\ cal}$ value was not in good agreement with the experimental value of $q_{e\ exp}$. These observations suggested that the pseudo-first-order model is not suitable for modeling the adsorption of Cr(VI) onto almond shell, activated sawdust, and activated carbon.

Pseudo-second-order model

The pseudo-second-order model is based on the assumption that the rate-limiting step is chemical sorption or chemisorption involving valence forces through sharing or exchange of electrons between sorbent and sorbate as covalent forces (Ofomaja 2008; Aharoni and Sparks 1991). The model has the following form (Chen et al. 2010):

$$\frac{dq}{dt} = k_2(q_e - q_t)^2 \tag{10}$$

where k_2 (g mg/min) is the rate constant of the second-order equation; q_e (mg/g) is the maximum adsorption capacity; q_t (mg/g) is the amount of adsorbed at time t (min).

After definite integration by applying the boundary conditions: $q_t = 0$ at $t = 0$ and $q_t = q_t$ at $t = t$, the Eq. 10 takes the form presented in Eq. 11:

$$\frac{t}{q_t} = \frac{1}{k_2 q_e^2} + \frac{t}{q_e} \tag{11}$$

If second-order kinetics is applicable, the plot of t/q_t against t showed a straight line; q_e and k_2 can then be obtained from the slope and intercept of the plot, respectively. For initial Cr(VI) concentration of 5 mg/L, k_2 and $q_{e\ cal}$ values along with the corresponding correlation coefficients are presented in Table 5. The correlation coefficient was nearly equal to unity and calculated $q_{e\ cal}$ value was very close to the experimental value of $q_{e\ exp}$. The results indicated that the pseudo-second-order adsorption mechanism is predominant for the adsorption of Cr(VI) onto almond shell, activated sawdust, and activated carbon,

Table 5 Calculated kinetic parameters for pseudo-first-order and second-order kinetic models for the adsorption of Cr(VI)

(mg/L) C_o	$q_{e\ exp}$ (mg/g)	Pseudo-first-order			Pseudo-second-order			Adsorbent name
		$q_{e\ cal}$ (mg/g)	k_1 (min^{-1})	R^2	$q_{e\ cal}$ (mg/g)	k_2 (g/mg/min)	R^2	
5	0.133	0.122	0.176	0.933	0.149	1.826	0.997	Almond shell
5	0.212	0.042	0.264	0.930	0.226	4.691	0.998	Activated carbon
5	0.227	0.130	0.125	0.983	0.256	1.131	0.999	Activated sawdust

and it is considered that the rate of the Cr(VI) adsorption process is controlled by the chemisorption process.

Thermodynamic studies

The standard Gibb's energy was calculated using Eq. 12 (Akmar Zakaria et al. 2009):

$$\Delta G^o = -RT \ln K_C \tag{12}$$

The equilibrium constant K_c was evaluated at each temperature using the following relationship:

$$K_C = \frac{C_{Ae}}{C_e} \tag{13}$$

where C_{Ae} is the amount adsorbed on solid at equilibrium and C_e is the equilibrium concentration (Han et al. 2006).

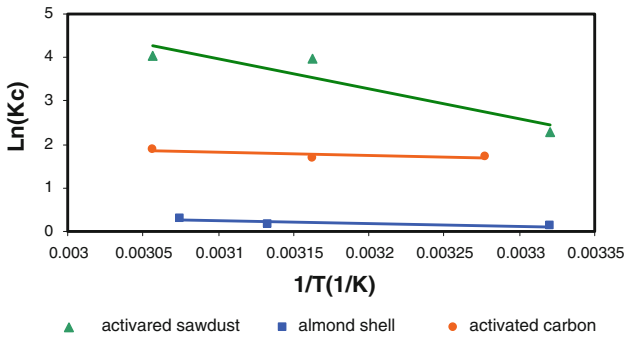

Fig. 9 Van't Hoff's plot at ambient temperature (initial Cr(VI) concentration = 5 mg/L, adsorbent dose = 2 g 100^{-1} mL, agitation speed = 400 rpm, contact time = 30 min)

The other thermodynamic parameters such as change in standard enthalpy (ΔH^o) and standard entropy (ΔS^o) were determined using the following equation:

$$\ln K_C = \frac{\Delta S^0}{R} - \frac{\Delta H^0}{RT} \tag{14}$$

ΔH^o and ΔS^o were obtained from the slope and intercept of the Van't Hoff's plot of $\ln K_c$ versus $1/T$ as shown in Fig. 9.

Positive value of ΔH^o indicates that the adsorption process is endothermic. The negative values of ΔG^o suggest the feasibility of the process. It was observed that the values become more negative with increase in temperature. Standard entropy determines the disorderliness of the adsorption at solid–liquid interface.

The values of ΔG^o, ΔH^o, and ΔS^o for the adsorption of Cr(VI) onto almond shell, activated sawdust, and activated carbon at different temperatures are given in Table 6.

The negative values of ΔG^o in the temperature range 28–50 °C were because of the adsorption process that was spontaneous and feasible, thermodynamically.

The values of ΔG^o decreased from −1.19 to −1.63 kJ mol^{-1} for almond shell, from −5.84 to −10.46 kJ mol^{-1} for activated sawdust, and from −4.00 to −4.73 kJ mol^{-1} for activated carbon with an increase in temperature from 28 to 50 °C, which indicates that the spontaneous nature of adsorption of Cr(VI) is inversely proportional to the temperature.

The positive values of ΔH^o suggested that the adsorption is endothermic, while the positive value of ΔS° indicates the randomness at the solid/solution interface during the

Table 6 Thermodynamic parameters of the Cr(VI) adsorption onto almond shell, activates sawdust and activated carbon at different temperatures

T (°C)	ΔG^0 (KJ mol^{-1})	ΔS^0 (J mol^{-1} K^{-1})	ΔH^0 (KJ mol^{-1})	Absorbent name
28	−1.49	20	4.83	Almond shell
40	−1.43			
50	−1.63			
28	−4.00	34	6.26	Activated carbon
40	−4.39			
50	−4.73			
28	−5.84	210	57.40	Activated sawdust
40	−8.36			
50	−10.46			

adsorption of Cr(VI) onto almond shell, activated sawdust, and activated carbon.

Conclusions

Almond shell and activated sawdust were found to be promising adsorbents for the uptake of Cr(VI) due to their low cost, easy availability, and high metal uptake capacity. The Cr(VI) removal efficiency of the almond shell, activated sawdust, and activated carbon was tested in the light of equilibrium, kinetics, and thermodynamics parameters. The kinetics of Cr(VI) adsorption onto almond shell, activated sawdust, and activated carbon followed the pseudo-second-order model. The results indicated that the data fit better to the Freundlich equation than to the Langmuir and Temkin equations. The thermodynamic parameters indicated that the adsorption of Cr(VI) onto almond shell, activated sawdust, and activated carbon was feasible, spontaneous, and endothermic.

The experimental results indicated that almond shell, activated sawdust, and activated carbon can be successfully used for the removal of Cr(VI) from aqueous solutions.

Acknowledgments The authors wish to thank Mr. Behrouz Baniasadi as well as Miss Toktam Sagharigar for their kind assistance in this research.

References

Abdel-Ghani NT, El-Chaghaby GA (2007) Influence of operating conditions on the removal of Cu, Zn, Cd and Pb ions from wastewater by adsorption. Int J Environ Sci Tech 4(4):451–456

Aharoni C, Sparks DL (1991) Kinetics of soil chemical reactions: a theoretical treatment. In: Sparks DL, Su′arez DL (eds) Rates of soil chemical processes. Soil Science Society of America, Madison, Wisconsin, pp 1–18

Akmar Zakaria Z, Suratman M, Mohammed N (2009) Chromium(VI) removal from aqueous solution by untreated rubber wood sawdust. Desalination 244:109–121

Aliabadi M, Morshedzadeh K, Soheyli H (2006) Removal of hexavalent chromium from aqueous solution by lignocellulosic solid wastes. Int J Environ Sci Tech 3(3):321–325

Arthur I, Vogel DS (1978) A text-book of quantitative inorganic analysis including elementary instrumental analysis, 4th edn. Longman, London

Bailey SE, Olin TJ, Bricka RM, Adrian DD (1999) A review of potentially low cost sorbents for heavy metals. Water Res 33:2469–2479

BianchiV Levis AG (1984) Mechanisms of chromium genotoxicity. Toxic Environ Chem 9:1–4

Chen DZ, Zhang JX, Chen JM (2010) Adsorption of methyl *tert*-butyl ether using granular activated carbon: equilibrium and kinetic analysis. Int J Environ Sci Tech 7(2):235–242

Feng D, Aldrich C (2004) Adsorption of heavy metals by biomaterials derived from the marine alga Ecklonia maxima. Hydrometallurgy 73:1–10

Gueu S, Yao B, Adouby K, Ado G (2007) Kinetics and thermodynamics study of lead adsorption on to activated carbons from coconut and seed hull of the palm tree. Int J Environ Sci Tech 4(1):11–17

Han R, Wang Y, Han P, Shi J, Yang J, Lu Y (2006) Removal of methylene blue from aqueous solution by chaff in batch mode. J Hazard Mater 137(1):550–557

Hasany SM, Chaudhary MH (1998) Fixation of Cr(III) traces onto Haro river sand from acidic solution. J Radioanal Nucl Chem 230:11–15

Karthikeyan T, Rajgopal S, Miranda LR (2005) Chromium (VI) adsorption from aqueous solution by Hevea Brasilinesis sawdust activated carbon. J Hazard Mater B124:192–199

Kozlowski CA, Walkowiak W (2002) Removal of chromium(VI) from aqueous solutions by polymer inclusion membranes. Water Res 36:4870–4876

Lagergren S (1898) About the theory of so-called adsorption of soluble substance. Kung Sven Veten Hand 24:1–39

Manal F (2007) Biosorption of cadmium and lead by phragmites Australis L. biomass using factorial experiment design. Glob J Biotech Biochem 2(1):10–20

Muradiye U, Irfan AR (2007) Removal of Cr(VI) from industrial wastewaters by adsorption: Part I: determination of optimum conditions. J Hazard Mater 149(2):482–491

Ofomaja AE (2008) Sorptive removal of methylene blue from aqueous solution using palm kernel fibre: effect of fibre dose. Biochem Eng J 40(1):8–18

Okoye AI, Ejikeme PM, Onukwuli OD (2010) Lead removal from wastewater using fluted pumpkin seed shell activated carbon: adsorption modeling and kinetics. Int J Environ Sci Tech 7(4):793–800

Ozaki H, Sharma K, Saktaywin W (2002) Performance of an ultra-lowpressure reverses osmosis membrane (ULPROM) for separating heavy metal: effects of interference parameters. Desalination 144:287–294

Shaalan H, Sorour M, Tewfik S (2001) Simulation and optimization of a membrane system for chromium recovery from tanning wastes. Desalination 14:315–324

Tunali Akar S, Yetimoglu Y, Gedikbey T (2009) Removal of chromium (VI) ions from aqueous solutions by using Turkish montmorillonite clay: effect of activation and modification. Desalination 244:97–108

Wuana RA, Okieimen FE, Imborvungu JA (2010) Removal of heavy metals from a contaminated soil using organic chelating acids. Int J Environ Sci Tech 7(3):485–496

Xi DL, Sun YS, Liu XY (1996) Environment monitor, vol 6. Advanced Education Press, Beijing, pp 2–3

Zavvar Mousavi H, Seyedi SR (2011) Nettle ash as a low cost adsorbent for the removal of nickel and cadmium from wastewater. Int J Environ Sci Tech 8(1):195–202

Zhang R, Wang B, Ma H (2010) Studies on Chromium (VI) adsorption on sulfonated lignite. Desalination 255:61–66